Applied Thermal Engineering 238 (2024) 122227

Contents lists available at ScienceDirect

Applied Thermal Engineering

journal homepage: www.elsevier.com/locate/apthermeng

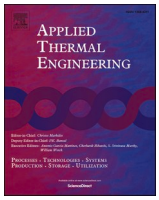

Research Paper

Performance evaluation of solar chimney in tunnel for passive ventilation and smoke exhaustion: A numerical approach

Youbo Huang [a,b], Bin Wang [a], Long Shi [b,*], Hua Zhong [c,*], Bingyan Dong [a]

[a] College of Safety Engineering, Chongqing University of Science and Technology, Chongqing 401331, China
[b] State Key Laboratory of Fire Science, University of Science and Technology of China, Hefei, Anhui 230026, China
[c] School of Architecture, Design and Built Environment, Nottingham Trent University, Nottingham NG1 4FQ, United Kingdom

ARTICLE INFO

Keywords:
Solar chimney
Natural ventilation
Tunnel fire
Smoke exhaustion
Renewable energy

ABSTRACT

Solar chimney applied in building ventilation can passively regulate indoor air quality without electricity cost and carbon emissions, but its application in tunnel is limited. This study conducted a numerical modelling and theoretical analysis to investigate the volumetric flow rate through multi-channel solar chimney group in tunnel under normal and fire conditions. The influences of the solar chimney arrangements on ventilation and smoke exhaustion capacity were analyzed. Results show that the solar chimney group can afford natural ventilation in tunnel without compromising the performance of smoke exhaustion through shaft. With absorbed more solar energy, increasing cavity amount and cavity width can effectively improve the ventilation performance but limited effect on smoke exhaustion. The volumetric flow rate increases with cavity height and cavity depth that is proportional to $h_c^{1/3}$ and $L^{2/3}$ under natural ventilation. The volumetric flow rate under natural ventilation and smoke exhaustion both increase with total chimney channel area. A theoretical model considering horizontally semi-parabolic temperature distribution inside each channel was developed to correlate the volumetric flow rate, the predictions agree reasonably with numerical results under normal and fire conditions. This study contributes to the application of solar chimney group in urban tunnels and guides extraction design.

1. Introduction

Energy usage and fire safety are inevitable considerations during the design and operation of urban tunnels [1]. Ventilation systems mainly dilute the vehicle pollutants inside the tunnel to keep their concentration under a safety threshold. On the other hand, those ventilation systems could also be adopted to exhaust the smoke if there occurs a fire. Tunnel fire is one of the critical hazards due to high-temperature smoke generated by fire [2], while statistical data show that heat and toxic smoke causes more than 85 % of the casualties in tunnel fires [3]. Therefore, a smoke exhaustion system is critical to improve the fire safety in tunnel. Currently, the smoke flow is controlled by mechanical ventilation and shaft ventilation in tunnel [4,5]. The longitudinal ventilation system consisted by jet fan is widely used due to their low construction cost and excellent performance. That the jet fan provides the driving force to push the polluted air and smoke towards to tunnel portals. However, this mechanical ventilation system consumes the electricity (68 % produced by fossil fuels). On the one hand, the related costs are quite high due to the long-time period operation and the continually increasing energy price [6]. On the other hand, consumption of fossil fuel raises energy crises and environmental problems due to pollution released during processing [7]. There is an urgent needed to adopt renewable energy system in tunnels for natural ventilation and smoke exhaustion.

Solar chimney, which is a shaft including a glazing wall to penetrate the solar radiation and a thermal absorption wall to heat the air in the chimney cavity, could be one of the ideal approaches to reduce energy consumption and enhance the fire safety of urban shallow tunnel [8]. The basic principle of solar chimney is based on the temperature gradient induced by solar irradiation [9]. As an economical and environmentally-friendly system, the solar chimney has been frequently applied in building ventilation to reduce the cost of the ventilation systems [10,11]. Due to the poor ventilation performance of solar chimney at night, the solar chimney always combines with the fan shaft system and phase-change materials to enhance the system performance [12 13] that not only saving energy but also achieving 24 h a day ventilation. Miyazaki *et al.* [14] argued that the fan shaft power requirement is reduced about 50 % in annual total in japan due to the natural ventilation based on solar chimney. Jaber and Ajib [15]

* Corresponding authors.
E-mail addresses: shilong@ustc.edu.cn (L. Shi), hua.zhong@ntu.ac.uk (H. Zhong).

https://doi.org/10.1016/j.applthermaleng.2023.122227
Received 22 August 2023; Received in revised form 15 November 2023; Accepted 12 December 2023
Available online 15 December 2023
1359-4311/© 2024 The Authors. Published by Elsevier Ltd. This is an open access article under the CC BY license (http://creativecommons.org/licenses/by/4.0/).

Nomenclature

A	area (m^2)
A_e	tunnel opening area (m^2)
A_i	inlet area (m^2)
$A_{i,j}$	inlet area of channel j (m^2)
A_o	outlet area (m^2)
$A_{o,j}$	outlet area of channel j (m^2)
A^*	area coefficient
B	buoyancy flux (m^4/s^3)
C_d	coefficient of discharge
c_p	specific heat (J/kg·K)
d_s	smoke thickness
E	power of heating source (W)
E_{d+1}	smoke heat source downstream of solar cavity channel d (W)
E_j	power of smoke through cavity j (W)
E_s	power of smoke (W)
g	gravitational acceleration (m/s^2)
h_c	chimney cavity height (m)
H	height (m)
H_c	height of channel (m)
H_e	height of tunnel entrance center (m)
H_t	height of tunnel ceiling (m)
$\triangle H$	height difference (m)
L	cavity depth (m)
N	amount of cavity in solar chimney group
P	pressure (Pa)
P_{e1}	pressure out of tunnel entrance (Pa)
P_{e2}	pressure at tunnel entrance (Pa)
P_{i1}	pressure external inlet (Pa)
P_{i2}	pressure internal inlet (Pa)
P_{o1}	pressure internal outlet (Pa)
P_{o2}	pressure enteral outlet (Pa)
$\triangle P$	pressure difference (Pa)
Q	heat release rate (kW)
T	temperature (K)
T_t	temperature in tunnel (K)
T_∞	ambient temperature (K)
T_{max}	maximum temperature (K)
$\triangle T_{max}$	maximum temperature rise (K)
$\triangle T_{max,i}$	maximum temperature rise at inlet (K)
u_s	maximum smoke flow velocity (m/s)
U	velocity (m/s)
U_e	velocity at tunnel entrance (m/s)
U_i	velocity at inlet (m/s)
U_o	velocity at outlet (m/s)
V	volumetric flow rate (m^3/s)
V_e	volumetric flow rate at tunnel entrance (m^3/s)
V_i	volumetric flow rate at inlet (m^3/s)
V_o	volumetric flow rate at outlet (m^3/s)
w	width (m)
wc	solar cavity width (m)
wt	tunnel width (m)
x	distance (m)
x_i	distance to inlet (m)
x_o	distance to reference position (m)

Greek symbols

$\triangle$	difference
κ	constant
ρ	density (kg/m^3)
ρ_c	density in solar cavity channel (kg/m^3)
ρ_s	smoke density (kg/m^3)
ρ_t	density in tunnel (kg/m^3)
ρ_∞	ambient density (kg/m^3)

Subscripts and Superscripts

∞	ambient condition
c	chimney cavity
d	downstream cavity serial number
e	tunnel opening
i	inlet
j	number
o	cavity outlet
t	tunnel
max	maximum
s	smoke

Abbreviation

NV	natural ventilation
SE	smoke exhaustion

obtained that the 32.1 % energy can be saved annually due to use the solar chimney for a residential building.

The main challenge of solar chimney applied in the building ventilation is to optimize its performance [16]. Long *et al.* [17] addressed the window configuration on natural ventilation performance of solar chimney applied in building. Hou et al.[18] experimentally studied the temperature distribution and airflow characteristic through one house solar chimney. The external radiation, temperature, and wind are important factors affecting the chimney cavity's airflow rate. Zhang et al. [19] argued the greater solar radiation would improve the airflow rate inside solar chimney cavity. Martínez *et al.* [20] suggested that external wind affects the ventilation performance of solar chimney in building. Divided the solar chimney cavity into multiple channels could improve the natural ventilation rate significantly [21]. Gong *et al* [22] suggested that split the solar chimney into multiple channels could increase ventilation rate by 57 %.

The solar chimney cannot only for operation ventilation but also for smoke exhaustion. Ding *et al.* [8] initiated the idea of applying the solar chimney in building smoke exhaustion. Cheng *et al.* [1] experimentally confirmed the viability of solar chimney in buildings considering both the function of natural ventilation and smoke exhaustion. Shi *et al.* [6] conducted the world-first study for solar chimney applied in a real building taking the natural ventilation and smoke exhaustion into account. The optimized designed of solar chimney in building natural ventilation has been extensively studied [23], but both considering natural ventilation and smoke exhaustion is still limited. The smoke exhaustion performance based on the solar chimney may be better than those of conventional shaft as it can combine the natural ventilation and enhance the thermal buoyance. That provides the possibility to transform the existing smoke exhaust shaft into a solar chimney to reduce the construction cost and energy saving.

The application of solar chimney in building natural ventilation and smoke exhaustion has been investigated [6]. The research on its applied in tunnel a long-narrow underground space is limited that impedes its practical application in tunnels. Cheng et al. validated the application of solar chimney in urban tunnel for both natural ventilation and smoke exhaustion [24]. Huang et al experimentally studied the natural ventilation performance of solar chimney in tunnel under varied solar radiation [7]. Solar chimney can be combined with urban tunnels' existing shaft system as it usually a few meters' shaft below the ground, such as the Wuhan Donghu Tunnel in China and the Nanjing Xi'an men Tunnel [25]. The passive solar energy adopted to the natural shaft group in

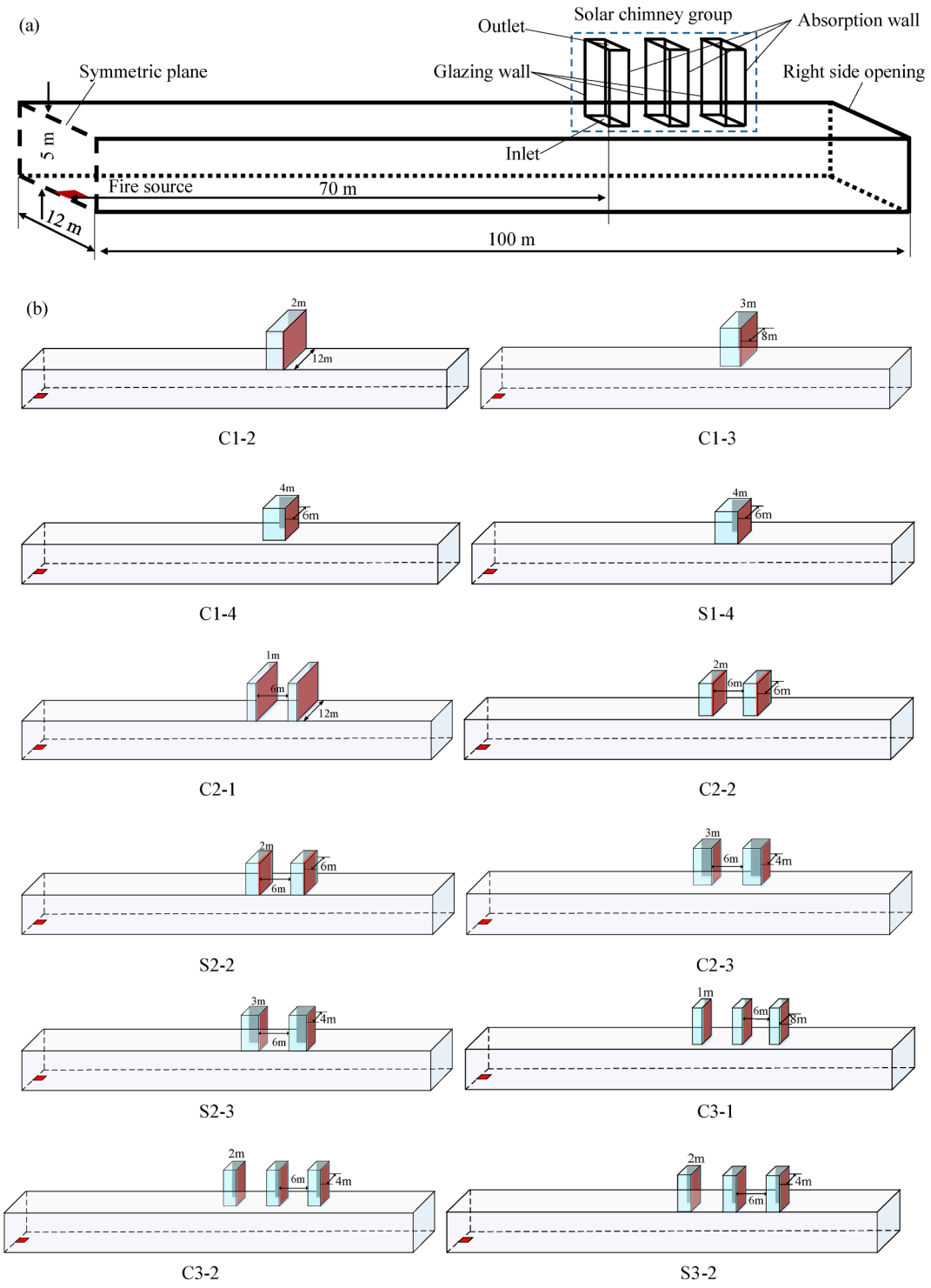

Fig. 1. Layout of the solar chimney in the tunnel: (a) schematic of tunnel model, (b) solar chimney groups.

tunnel not only effectively exhausting smoke but also enhancing the air flow under normal condition, such as solar chimney adopted to Leijiapo No.1 Tunnel in Shanxi, China. However, the solar chimney application in tunnels with groups of several ventilation shafts have not been revealed both under natural ventilation and smoke exhaustion. In addition, the influences of the shaft groups arrangement, chimney configuration, and fire scenario on the performance of solar chimney group is different from house buildings. The related theoretical model and optimum building design parameters may not apply to tunnels. It is necessary to investigate the optimum performance of solar chimney group in the tunnel and develop the related theoretical model.

In view of this, the present work investigated the performances of solar chimney group applied in the tunnel, considering both natural ventilation and smoke exhaustion under normal and fire conditions. A series of numerical cases were conducted with different shaft groups arrangement to discuss the performance of ventilation and smoke exhaustion, and a theoretical model is developed to fill the gap. This work aims to provide brand-new concept of tunnel ventilation and can be solved by hand to reduce design costs.

Table 1
Test conditions.

No.	Group name	Cavity amounts	L (m)	w (m)	Solar radiation (W/m^2)	Fire size (MW)
1-4	C1-2	1	2	12	400, 800, 1200	0, 3, 10, 20
5-8	C1-3	1	3	8		
9-12	C1-4	1	4	6		
13-16	S1-4	1	4	6		
17-20	C2-1	2	1	12		
21-24	C2-2	2	2	6		
25-28	S2-2	2	2	6		
29-32	C2-3	2	3	4		
33-26	S2-3	2	3	4		
37-40	C3-1	3	1	8		
41-44	C3-2	3	2	4		
45-48	S3-2	3	2	4		

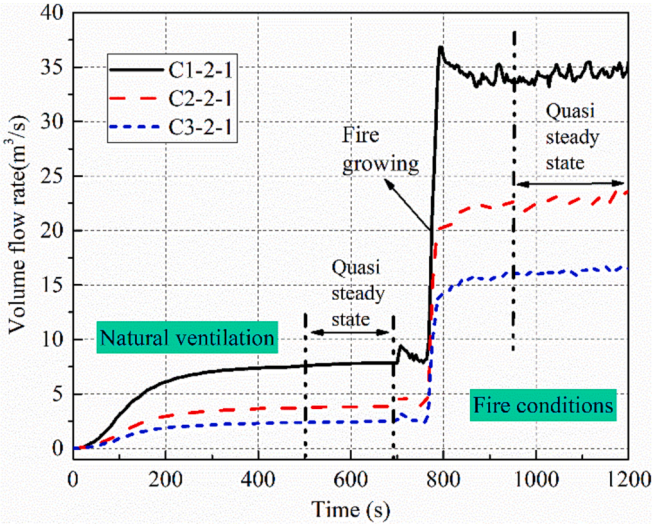

Fig. 2. Volumetric flow rate in solar chimney.

2. Numerical methodology

2.1. Numerical scenarios

The performance of the solar chimney for natural ventilation and smoke exhaustion are investigated using a numerical software package, namely FDS (Fire Dynamics Simulator). FDS is a practical computational fluid dynamics (CFD) model of fire-driven fluid flow developed by NIST (the U.S. National Institute of Standards and Technology). FDS numerically solves a form of the Navier-Stokes equations appropriate for low-speed (Ma < 0.3), thermally-driven flow with an emphasis on smoke and heat transport from fires, as well as the heating, ventilation, and air conditioning (HVAC). The validation of FDS for solar chimney in ventilation has been verified and validated [1,20]. A sub grid-scale stress model was used to precisely calculate the flow field viscous stress. The Smagorinsky Deardorff's model was adopted to deal the turbulence.

The numerical model was constructed through FDS based on the three-lane tunnel [26]. Total of 200 m length tunnel symmetrical at fire source was considered. In order to save the computational time, a symmetric plane is employed [27], as shown in Fig. 1 (a). Therefore, the tunnel with 100 m length (12 m width, 5 m height) in fire source one side was selected for the present analysis, where the influence of tunnel length on solar chimney performance can be ignored [24].

The solar chimney, including only single cavity, two and three identical cavities arranged in a group at intervals of 6 m, are installed at top of the tunnel. The cavity height was 5 m. The cavity depth (1 m-4 m) and cavity width (4 m-12 m) vary for each identical cavity under the same total opening area. The solar chimney was arranged at the tunnel ceiling center and the ceiling side when the cavity width was not greater than 6 m. A total of 12 groups of the solar chimney layout are considered naming as C*n*-*m*-*d* or S*n*-*m*-*d*, where "C" and "S" represent the centerline and sideline, respectively, as shown in Fig. 1 (b). The symbol n is the amount of cavity in the group, and m is the individual cavity depth, and d is the designative cavity number in the group which increases further from the fire source. The sidewall, ceiling and bottom plate of tunnel was constructed with "concrete" (density of 2280 kg/m^3, thermal conductivity of 1.8 W/(m·K), specific heat of 1.04 kJ/(kg·K)). The left sidewall of the solar chimney was made with glass (conductivity 1.2 W / (m·K)). The right sidewall of solar chimney was covered with aluminum (density of 2700 kg/m^3, thermal conductivity of 167 W/(m·K), specific heat of 0.1 kJ/(kg·K), emissivity of 0.95) to absorb the solar radiation. The boundary of the computational domain was set as an "open".

The fire source (3 MW, 10 MW, 20 MW) was located at the tunnel centerline. The distance between the fire source and solar chimney left side was 70 m. The solar radiation 400 W/m^2, 800 W/m^2, 1200 W/m^2 [28] was carried out under normal condition. Due to incomparable between solar radiation to fire power and inconspicuous impact of solar radiation on smoke exhaustion [1,20], the solar intensity 800 W/m^2 were conducted under fire conditions. Table 1 lists the test cases. The average data of air and smoke flow rate at stable period are sued for

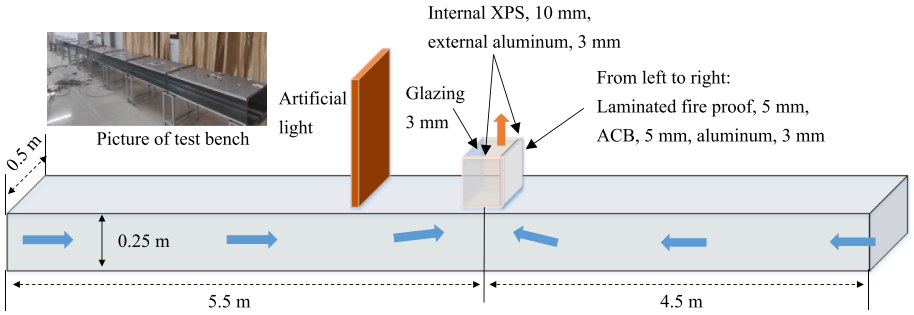

Fig. 3. A schematic of solar chimney experimental test platform.

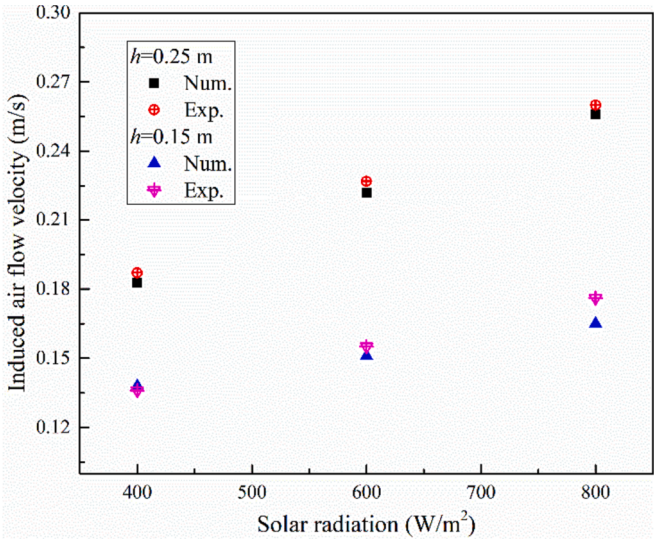

Fig. 4. A comparison of average flow rate inside cavity.

following analysis, as shown in Fig. 2.

2.2. Validation of numerical tool

2.2.1. Validated using experimental results

The experiment conducted on a model tunnel with dimension of 10 m (L) × 0.5 m (W) × 0.25 m (H) was used to validate the numerical result [7], as shown in Fig. 3. The width of the chimney cavity (w) was 15 cm, and cavity depth (d) is 10 cm (all internal sizes). Two cavity heights (h) (15 cm, 25 cm) and three solar radiation intensity (400 W/m^2, 600 W/m^2, 800 W/m^2) were carried out. The detail description of experiment can be seen in reference [21].

The numerical model, same with the reduced scale experiment, was carried out. The numerical results of airflow velocity through the channel are compared with the experimental data as shown in Fig. 4. The average absolute errors between numerical results and experimental data is 0.5 %, which is accepted. The viability of FDS addressing tunnel fire and smoke exhaustion has been extensively confirmed. Therefore, FDS can be used to analyze the performance of solar chimney in tunnels both under natural ventilation and fire conditions.

2.2.2. Grid independence analysis

Grid sensitivity analysis is important in numerical simulation as it can influence the calculation accuracy and numerical results. The grid size is related to the characteristic length (D^*), and always obtains accurate result with grid size equal to $0.1D^*$ [25]. The corresponding grid sizes under $0.1D^*$ is 0.15 m for the minimum heat release rate of 3 MW. Thus, four different grid sizes were conducted to examine the grid independence including 0.1 m, 0.2 m, 0.3 m, and 0.4 m. The solar groups of C3-2 and solar radiation of 800 W/m^2 were conducted for grid analysis. Fig. 5 shows the volume flow rate through C3-2–1 and C3-2–2. The volume flow rate gets very close for grid size less than 0.3 m. The accuracy of 0.2 m grid size has also been validated for shaft smoke exhaustion in the tunnel with a dimension of 12 m (H) and 5 m (W) [27]. Therefore, the grid size of 0.2 m is chosen for this study.

3. Analytical model

3.1. Theoretical model for natural ventilation

Fig. 6 shows the solar chimney arrangement installed on the tunnel roof under natural ventilation. In this study, it is assumed that (a) the air

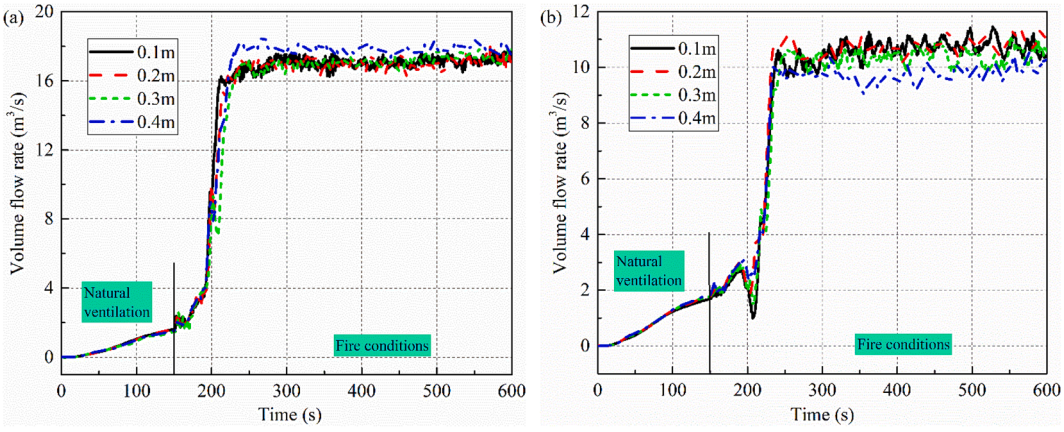

Fig. 5. Volume flow rate under different grid sizes with C3-2, E = 800 W/m^2, Q = 3 MW: (a) airflow through C3-2–1, (b) airflow through C3-2–3.

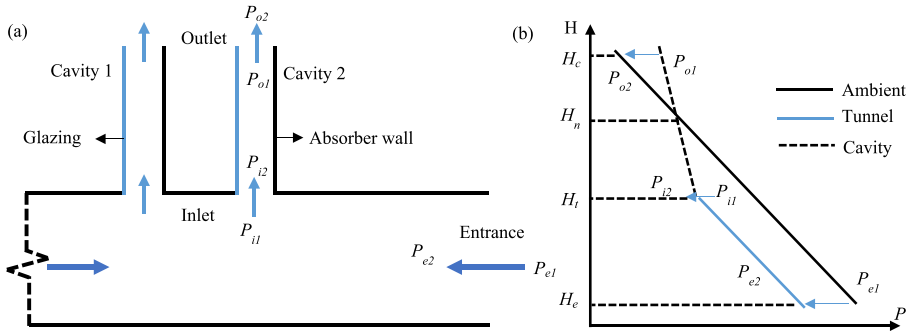

Fig. 6. Solar chimney group under natural ventilation: (a) schematic of airflow, (b) the pressure distribution.

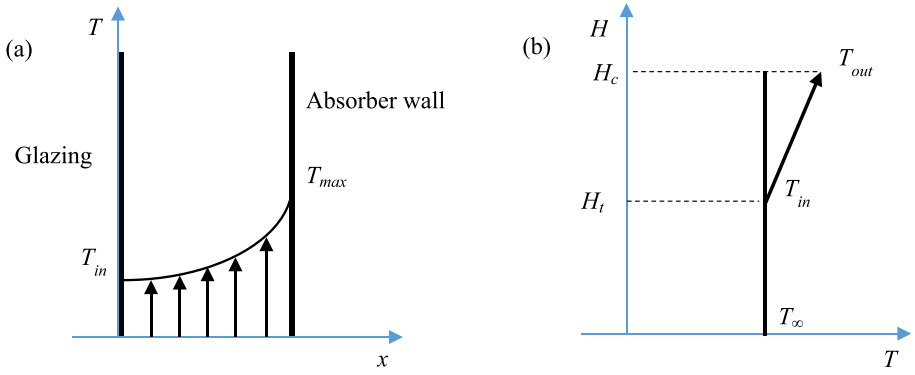

Fig. 7. Semi parabolic temperature distribution inside solar chimney: (a) temperature in horizontal direction, (b) temperature in vertical direction.

inside the cavity, tunnel environment and outdoor environment are well mixed and uniform, hydrostatic pressure is considered linearly varied with height; (b) the discharge coefficients for all the orifices are considered the same; (c) the friction losses are ignored due to the complexity of the problem; (d) the external wind in the outdoor environment is neglected; and (e) this study much focuses on predicting solar chimney performance under steady status, where there is a balance of heat transfer between the walls and airflow; (f) the volumetric flow rate through each cavity in solar chimney group is same under natural ventilation.

The solar energy absorbed by the absorption wall enhances pressure drop because of the greater density difference between orifice two sides. The pressure drop induces on the basis of height difference and density change, which can be expressed by Eq. (1). The inside air is heated by solar energy, the slope of pressure decay rate inside cavity is slower both than outer and in tunnel, as shown in Fig. 6 (b), where H_n is the height of neutral plane. Due to the solar chimney at the top of tunnel, the pressure curve in cavity is above the tunnel. The pressure distribution in tunnel and outdoor can be presented using parallel lines. The neutral pressure planes only occurred in cavity. This is different with previous study [24] that assumed tunnel as infinite space.

$$\Delta P = \rho g \Delta H \tag{1}$$

The pressure difference drives the air through orifices, including the tunnel opening, cavity inlet and outlet. The relationship between the airflow velocity and pressure difference can be expressed as,

$$\Delta P = \frac{1}{2}\rho U^2 \tag{2}$$

The pressure difference at the tunnel opening, cavity inlet and outlet can be obtained by following formulas.

$$P_{e1} - P_{e2} = \frac{1}{2}\rho_\infty U_e^2 \tag{3}$$

$$P_{e2} - P_{i1} = \rho_t g(H_t - H_e) \tag{4}$$

$$P_{i1} - P_{i2} = \frac{1}{2}\rho_t U_i^2 \tag{5}$$

$$P_{i2} - P_{01} = \rho_c g(H_c - H_t) \tag{6}$$

$$P_{01} - P_{02} = \frac{1}{2}\rho_c U_0^2 \tag{7}$$

The pressure gradient between P_{e1} and P_{o2} can be given by Eq. (8).

$$P_{e1} - P_{02} = \rho_\infty g(H_c - H_e) \tag{8}$$

Based on the Eq. (3) to Eq. (8), it is obtained,

$$\rho_\infty U_e^2 + \rho_t U_i^2 + \rho_c U_0^2 = 2\rho_\infty g(H_c - H_e) - 2\rho_t g(H_t - H_e) - 2\rho_c g(H_c - H_t) \tag{9}$$

The conservation of mass can be given by,

$$\rho_\infty V_e = N\rho_t V_i = N\rho_c V_o \tag{10}$$

The volumetric flow rate through the orifice can be calculated by,

$$V_i = C_d A_i U_i \tag{11}$$

Based on the volumetric flow rate and mass flux expression, Eq. (9) can be simplified and obtained the air flow rate at inlet.

$$U_i = \sqrt{\frac{A_e^2 A_o^2 (2\rho_\infty g(H_c - H_e) - 2\rho_t g(H_t - H_e) - 2\rho_c g(H_c - H_t))}{\frac{\rho_t^2 N^2 A_i^2 A_o^2}{\rho_\infty} + \frac{\rho_t^2 A_i^2 A_e^2}{\rho_c} + \rho_t A_e^2 A_o^2}} \tag{12}$$

The temperature rise inside tunnel is small enough to ignored, thus, it can be assumed $\rho_t = \rho_\infty$. Furtherly, it is assumed that neglected the density difference excepting density defect calculation $(\rho\text{-}\rho_\infty)gh$, thus, Eq. (12) can be simplified as,

$$U_i = \sqrt{\frac{A_e^2 A_o^2 2g(\rho_\infty - \rho_c)(H_c - H_t)}{(N^2 A_i^2 A_o^2 + A_i^2 A_e^2 + A_e^2 A_o^2)\rho_c}} \tag{13}$$

Based on the ideal gas law $\rho_\infty T_\infty = \rho_t T_t = \rho_c T_c$, Eq. (13) furtherly simplified as,

$$U_i = \sqrt{\frac{A_e^2 A_o^2 2g(T_c - T_\infty)(H_c - H_t)}{(N^2 A_i^2 A_o^2 + A_i^2 A_e^2 + A_e^2 A_o^2)T_\infty}} \tag{14}$$

The temperature nearby the absorption wall is higher than that near glazing wall [25–27]. For cavity depth exceeding the order of centimeters, the temperature decreased from heated wall to glazing side due to convective heat transfer and one side heat source [29–31]. The horizontal temperature inside the solar chimney is considered as semi parabolic decay that is more fitted practice, as shown in Fig. 7. Thus, the temperature along with the cavity depth can be expressed as Eq. (15).

$$T = \frac{T_{max} - T_\infty}{L^{3/2}} x^{3/2} + T_\infty \tag{15}$$

Substituted temperature expression into Eq. (14), the volumetric flow rate can be given by,

$$V_i = \int_0^L C_d w_c \sqrt{\frac{A_e^2 A_o^2 2g(T_{max} - T_\infty)(H_c - H_t)}{(N^2 A_i^2 A_o^2 + A_i^2 A_e^2 + A_e^2 A_o^2)L^{3/2} T_\infty}} x^{3/4} dx \tag{16}$$

From previous study [24], the total absorbed energy can be given by Eq. (17).

$$E = \int_0^L \kappa (T - T_\infty)^{\frac{3}{2}} dx, \kappa = w_c \rho_\infty c_p C_d \sqrt{\frac{g h_c}{T_\infty}} \tag{17}$$

Substitute Eq. (15) into Eq. (17), the total energy is expressed by,

$$E = \frac{4}{13}\kappa (T_{max} - T_\infty)^{\frac{3}{2}} L \tag{18}$$

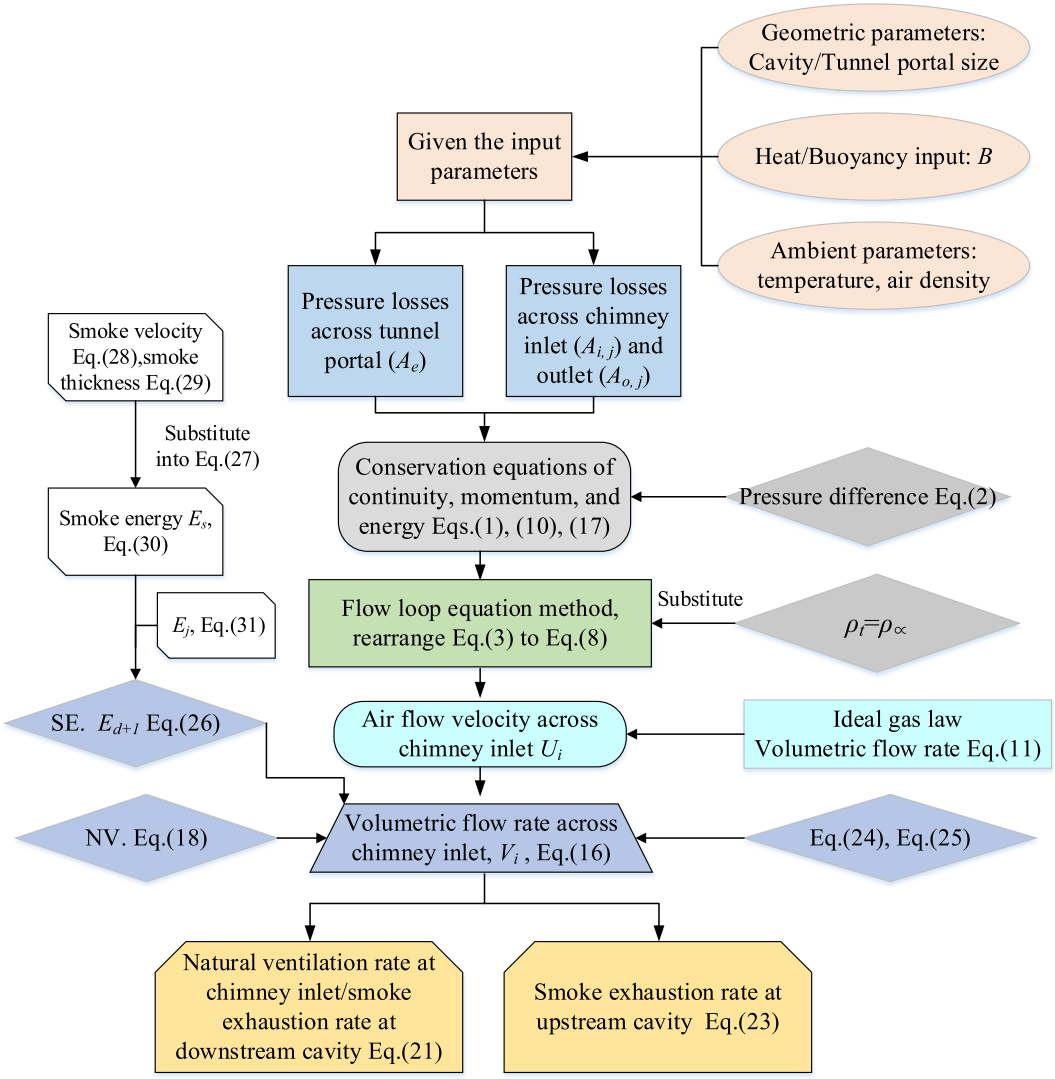

Fig. 8. Flow chart for theoretical modelling. NV. means natural ventilation, SE. means smoke exhaustion.

The total solar energy absorbed by wall is used to heat the inside air. Under the steady condition, the volumetric flow rate can be simplified as following Eq. (19).

$$V_i = 0.846(C_d w_c L)^{2/3}\sqrt{\frac{2A_e^2A_o^2}{(N^2A_i^2A_o^2 + A_i^2A_e^2 + A_e^2A_o^2)}}(Bh_c)^{1/3} \tag{19}$$

where B is the buoyancy flux, which driven airflow inside chimney cavity,

$$B = \frac{Eg}{T_\infty c_p \rho_\infty} \tag{20}$$

The vertically liner temperature distribution is considered with coefficient 0.794 in previous study [24]. The volumetric flow rate at the inlet can be expressed as Eq. (21) considering vertically liner temperature distribution and horizontally semi parabolic temperature distribution.

$$V_i = 0.672(C_d w_c L)^{2/3} A^*(Bh_c)^{1/3} \tag{21}$$

where A^* is the coefficient considering the tunnel and chimney cavity configuration given by,

$$A^* = \sqrt{\frac{2A_e^2A_o^2}{(N^2A_i^2A_o^2 + A_i^2A_e^2 + A_e^2A_o^2)}} \tag{22}$$

3.2. Theoretical model for smoke exhaustion

The smoke exhaustion in solar chimney cavity is promoted by two parts heat source: high temperature smoke from fire source and solar radiation. The hot smoke coming from upstream side of chimney cavity, thus, the smoke exhausted through upstream cavity is more than that downstream. The smoke exhaustion rate through chimney cavity can be predicted using Eq. (16), where the maximum smoke temperature beneath the tunnel ceiling should be as maximum value at the inlet. Eq. (16) can be simplified as,

$$V_i = \frac{4}{7} w_c L C_d A^* \sqrt{\frac{g h_c \Delta T_{max,i}}{T_\infty}} \tag{23}$$

where $\triangle T_{max,i}$ is the temperature rise at inlet, which can be correlated using sum of two exponential equations based on the maximum temperature beneath the tunnel ceiling,

$$\frac{\Delta T_{\max,i}}{\Delta T_{\max}} = 0.55\exp(-0.143\frac{x_i - x_0}{H_t}) + 0.45exp(-0.024\frac{x_i - x_0}{H_t}) \tag{24}$$

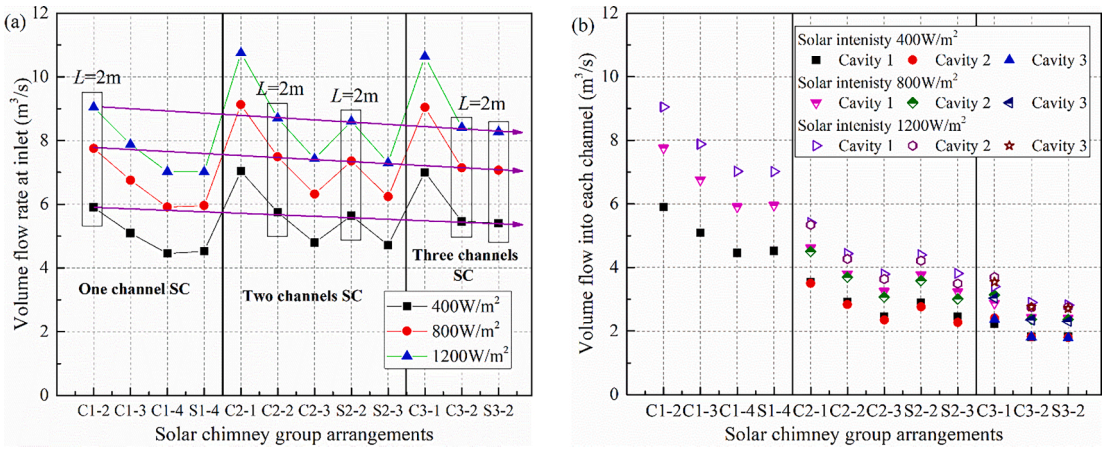

Fig. 9. Volume flow rate under different conditions: (a) total airflow, (b) airflow in each channel.

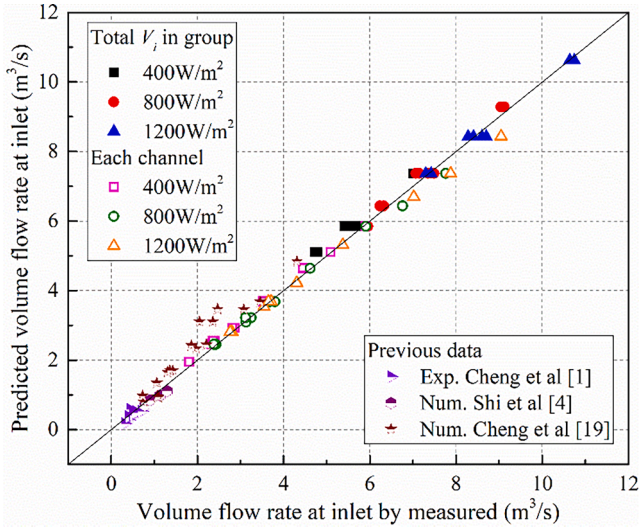

Fig. 10. Comparison of natural ventilation measured experimentally, numerically and analytical model.

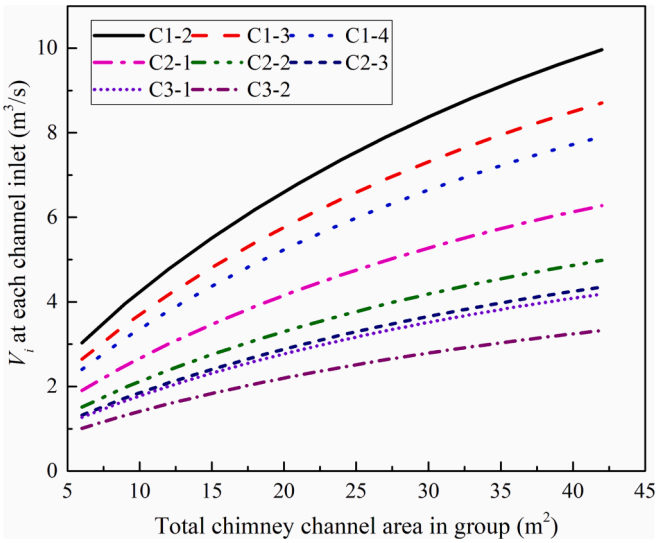

Fig. 12. Variation of natural ventilation rate with total chimney cavity area.

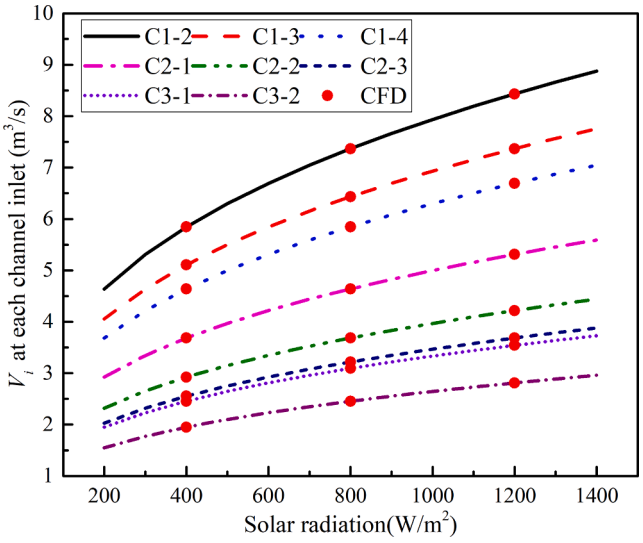

Fig. 11. Variation of natural ventilation rate with solar radiation.

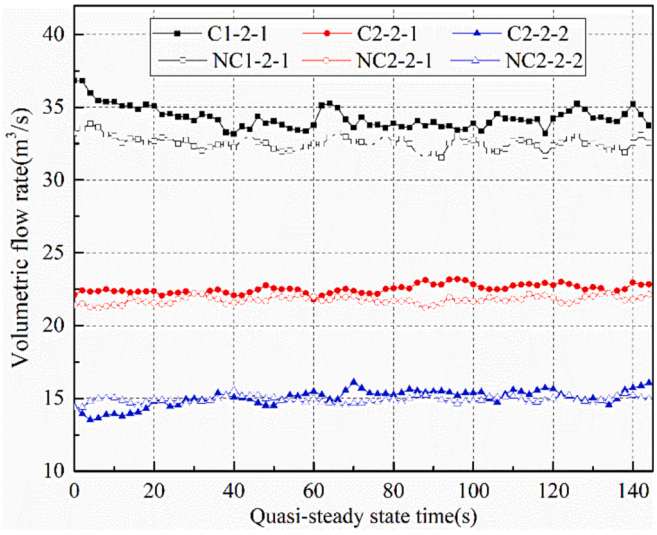

Fig. 13. Volumetric flow rate inside channel with and without solar radiation.

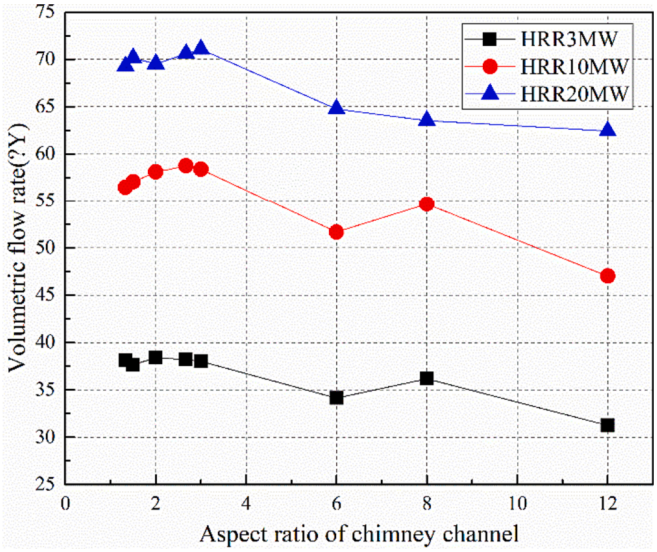

Fig. 14. Smoke flow rate at inlet under varied AR of chimney channel.

where x_i is the longitudinal position at inlet, x_o is the reference position of maximum temperature beneath the tunnel ceiling, $\triangle T_{max}$ is the maximum temperature rise beneath the tunnel ceiling.

Li *et al.* [32] developed an empirical model to predict the maximum temperature rise beneath the tunnel ceiling for dimensionless ventilation velocity less than 0.19, expressed as,

$$\Delta T_{max} = 17.5\frac{Q^{2/3}}{H_t^{5/3}} \tag{25}$$

Substituted Eq. (25) into Eq. (24) can predict the temperature rise at the inlet, then substituted Eq. (24) into Eq. (23) can calculate the smoke exhaustion rate at upstream cavity inlet.

For the smoke exhaustion through the downstream cavity in the solar chimney group, the smoke flow is driven by two parts: the heat source of downstream smoke and solar radiation. Based on the energy conservation, the downstream smoke heat source can be given by,

$$E_{d+1} = E_s - \sum_1^d E_j \tag{26}$$

The part of energy provided from hot smoke can be given by

$$E_s = \rho_s u_s w_t d_s c_p \Delta T_{\max} \tag{27}$$

The maximum smoke flow velocity can be predicted based on the density difference [33], given by

$$u_s = 0.613\left(gH_t\frac{\Delta T_{\max}}{T_{\max}}\right)^{1/2} \tag{28}$$

The smoke stratification in one-dimensional region can be assumed steady. Oka *et al.* [34] developed a model to predict the smoke thickness d_s in the tunnel, expressed as follows.

$$\frac{d_s}{H_t} = 0.266\left(\frac{\pi}{2}\right)^{-2/3}\left(\frac{w_t}{2H_t}\right)^{-1/3} \tag{29}$$

Based on the ideal gas law, substituted Eq. (28) and Eq. (29) into Eq. (27), the power of smoke layer can be expressed as,

$$E_s = 0.613\rho_\infty T_\infty\left(\frac{\Delta T_{\max}}{T_{\max}}\right)^{3/2}(gH_t)^{1/2}w_t d_s c_p \tag{30}$$

Based on the ideal gas law and volumetric flow rate of cavity j, the

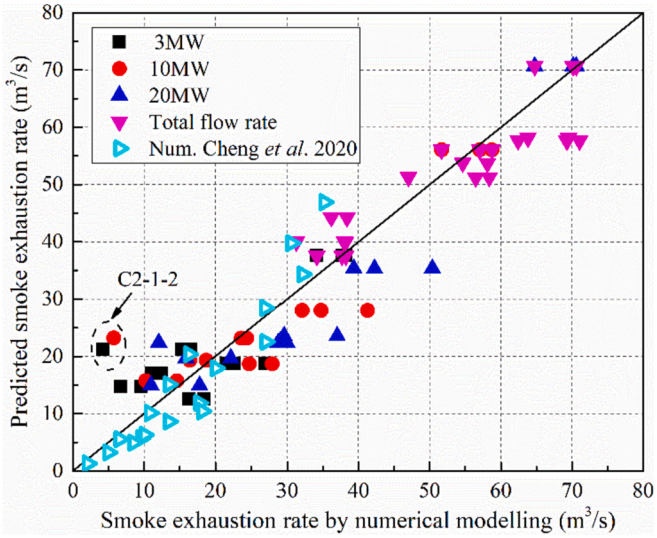

Fig. 16. A comparison of smoke exhaustion rate by analytical model and numerical result.

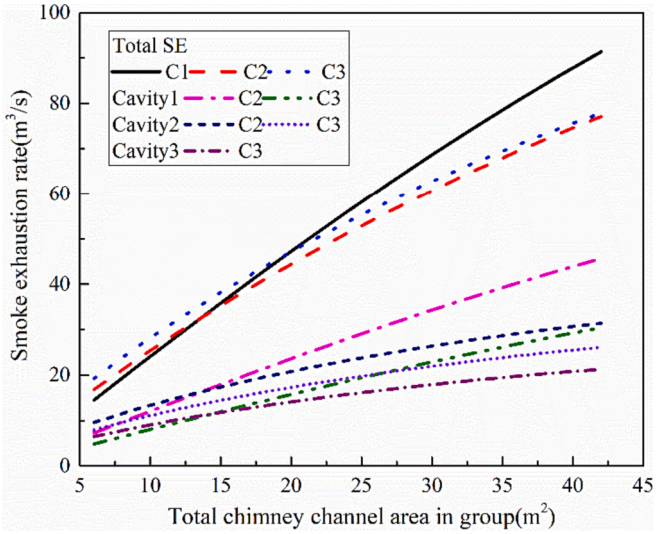

Fig. 17. Smoke exhaustion versus Total chimney channel area.

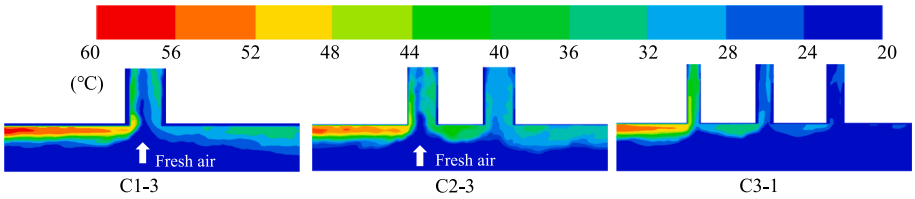

Fig. 15. Temperature distribution in tunnel center and channels under fire size 3 MW.

Table A1
Natural ventilation rate under solar radiation 400 W/m$^{2.}$

Scenario No.	Location	Cavity depth, width	AR of cavity	E (W/m^2)	Volume flow rate (m^3/s)			
					Cavity 1#	Cavity 2#	Cavity 3#	Total
C1-2	1 center vent	2 m × 12 m	6	400	5.90	–	–	5.9
C1-3	1 center vent	3 m × 8 m	8/3		5.09	–	–	5.09
C1-4	1 center vent	4 m × 6 m	1.5		4.45	–	–	4.45
S1-4	1 side vent	4 m × 6 m	1.5		4.52	–	–	4.52
C2-1	2 center vents	1 m × 12 m	12		3.54	3.50	–	7.04
C2-2	2 center vents	2 m × 6 m	3		2.92	2.83	–	5.75
C2-3	2 center vents	3 m × 4 m	4/3		2.45	2.35	–	4.8
S2-2	2 side vents	2 m × 6 m	3		2.88	2.76	–	5.64
S2-3	2 side vents	3 m × 4 m	4/3		2.45	2.27	–	4.72
C3-1	3 center vents	1 m × 8 m	8		2.23	2.41	2.37	7.01
C3-2	3 center vents	2 m × 4 m	2		1.82	1.82	1.82	5.46
S3-2	3 side vents	2 m × 4 m	2		1.83	1.80	1.78	5.41

Table A2
Natural ventilation rate under solar radiation 800 W/m$^{2.}$

Scenario No.	Location	Cavity depth, width	AR of cavity	E (W/m^2)	Volume flow rate (m^3/s)			
					Cavity 1#	Cavity 2#	Cavity 3#	Total
C1-2	1 center vent	2 m × 12 m	6	800	7.76	–	–	7.76
C1-3	1 center vent	3 m × 8 m	8/3		6.76	–	–	6.76
C1-4	1 center vent	4 m × 6 m	1.5		5.91	–	–	5.91
S1-4	1 side vent	4 m × 6 m	1.5		5.96	–	–	5.96
C2-1	2 center vents	1 m × 12 m	12		4.62	4.50	–	9.12
C2-2	2 center vents	2 m × 6 m	3		3.80	3.69	–	7.49
C2-3	2 center vents	3 m × 4 m	4/3		3.25	3.07	–	6.32
S2-2	2 side vents	2 m × 6 m	3		3.77	3.59	–	7.36
S2-3	2 side vents	3 m × 4 m	4/3		3.23	3.00	–	6.23
C3-1	3 center vents	1 m × 8 m	8		2.87	3.13	3.04	9.04
C3-2	3 center vents	2 m × 4 m	2		2.43	2.37	2.35	7.15
S3-2	3 side vents	2 m × 4 m	2		2.40	2.36	2.30	7.06

Table A3
Natural ventilation rate under solar radiation1200W/m$^{2.}$

Scenario No.	Location	Cavity depth, width	AR of cavity	E (W/m^2)	Volume flow rate (m^3/s)			
					Cavity 1#	Cavity 2#	Cavity 3#	Total
C1-2	1 center vent	2 m × 12 m	6	1200	9.05	–	–	9.05
C1-3	1 center vent	3 m × 8 m	8/3		7.88	–	–	7.88
C1-4	1 center vent	4 m × 6 m	1.5		7.02	–	–	7.02
S1-4	1 side vent	4 m × 6 m	1.5		7.01	–	–	7.01
C2-1	2 center vents	1 m × 12 m	12		5.41	5.34	–	10.75
C2-2	2 center vents	2 m × 6 m	3		4.44	4.27	–	8.71
C2-3	2 center vents	3 m × 4 m	4/3		3.79	3.63	–	7.42
S2-2	2 side vents	2 m × 6 m	3		4.39	4.21	–	8.6
S2-3	2 side vents	3 m × 4 m	4/3		3.81	3.49	–	7.3
C3-1	3 center vents	1 m × 8 m	8		3.4	3.69	3.54	10.63
C3-2	3 center vents	2 m × 4 m	2		2.9	2.75	2.75	8.4
S3-2	3 side vents	2 m × 4 m	2		2.82	2.75	2.71	8.28

Table A4
Smoke exhaustion rate under heat release rate 3 MW.

Scenario No.	Location	Cavity depth, width	AR of cavity	E (W/m^2)	Volume flow rate (m^3/s)			
					Cavity 1#	Cavity 2#	Cavity 3#	Total
C1-2	1 center vent	2 m × 12 m	6	800	34.13	0.00	0.00	34.13
C1-3	1 center vent	3 m × 8 m	8/3		38.22	–	–	38.22
C1-4	1 center vent	4 m × 6 m	1.5		37.67	–	–	37.67
S1-4	1 side vent	4 m × 6 m	1.5		35.52	–	–	35.52
C2-1	2 center vents	1 m × 12 m	12		27.07	–	–	31.25
C2-2	2 center vents	2 m × 6 m	3		22.67	15.34	–	38.01
C2-3	2 center vents	3 m × 4 m	4/3		21.60	16.56	–	38.16
S2-2	2 side vents	2 m × 6 m	3		21.36	13.91	–	35.27
S2-3	2 side vents	3 m × 4 m	4/3		20.02	15.51	–	35.53
C3-1	3 center vents	1 m × 8 m	8		18.40	11.04	–	36.18
C3-2	3 center vents	2 m × 4 m	2		16.27	12.47	9.63	38.37
S3-2	3 side vents	2 m × 4 m	2		14.70	10.10	10.16	34.96

Table A5
Smoke exhaustion rate under heat release rate 10 MW.

Scenario No.	Location	Cavity depth, width	AR of cavity	E (W/m^2)	Volume flow rate (m^3/s)			
					Cavity 1#	Cavity 2#	Cavity 3#	Total
C1-2	1 center vent	2 m × 12 m	6	800	51.67	–	–	51.67
C1-3	1 center vent	3 m × 8 m	8/3		58.76	–	–	58.76
C1-4	1 center vent	4 m × 6 m	1.5		57.06	–	–	57.06
S1-4	1 side vent	4 m × 6 m	1.5		54.46	–	–	54.46
C2-1	2 center vents	1 m × 12 m	12		41.27	5.75	–	47.02
C2-2	2 center vents	2 m × 6 m	3		34.73	23.66	–	58.39
C2-3	2 center vents	3 m × 4 m	4/3		32.07	24.41	–	56.48
S2-2	2 side vents	2 m × 6 m	3		31.97	21.06	–	53.03
S2-3	2 side vents	3 m × 4 m	4/3		29.23	21.84	–	51.07
C3-1	3 center vents	1 m × 8 m	8		27.99	16.44	10.22	54.65
C3-2	3 center vents	2 m × 4 m	2		24.78	18.72	14.61	58.11
S3-2	3 side vents	2 m × 4 m	2		21.09	14.20	14.39	49.68

Table A6
Smoke exhaustion rate under heat release rate 10 MW.

Scenario No.	Location	Cavity depth, width	AR of cavity	E (W/m^2)	Volume flow rate (m^3/s)			
					Cavity 1#	Cavity 2#	Cavity 3#	Total
C1-2	1 center vent	2 m × 12 m	6	800	64.76	–	–	64.76
C1-3	1 center vent	3 m × 8 m	8/3		70.59	–	–	70.59
C1-4	1 center vent	4 m × 6 m	1.5		70.15	–	–	70.15
S1-4	1 side vent	4 m × 6 m	1.5		0.00	–	–	0.00
C2-1	2 center vents	1 m × 12 m	12		50.37	12.05	–	62.42
C2-2	2 center vents	2 m × 6 m	3		42.27	28.80	–	71.07
C2-3	2 center vents	3 m × 4 m	4/3		39.32	29.95	–	69.27
S2-2	2 side vents	2 m × 6 m	3		0.00	0.00	–	0.00
S2-3	2 side vents	3 m × 4 m	4/3		0.00	0.00	–	0.00
C3-1	3 center vents	1 m × 8 m	8		36.98	15.89	10.96	63.83
C3-2	3 center vents	2 m × 4 m	2		29.55	22.18	17.78	69.51
S3-2	3 side vents	2 m × 4 m	2		28.80	18.51	19.20	66.51

power of smoke exhausted through cavity j can be given by

$$E_j = \frac{\rho_\infty T_\infty}{T_{\max,i}} V_{i,j} c_p \Delta T_{\max,j} \tag{31}$$

Substituted Eq. (31) into Eq. (26) to calculate E_{d+1}, then submitted $E_{d+1} + E$ into Eq. (20) to calculate the buoyance flux B, the volumetric flow rate through downstream cavity can be predicted by inserting this B into Eq. (21). The derivation process of induced volumetric flow rates entry solar chimney group inlet can refer to flowchart Fig. 8.

4. Results and discussion

4.1. Natural ventilation

4.1.1. Numerical results

Fig. 9 shows the volumetric flow rate of different solar chimney group arrangements and across each chimney channels in group. The greater solar radiation intensity not only enhanced the total airflow rate in groups but also for each channels due to stronger thermal buoyancy [18,20,32]. Under the same channel amounts in group, the total airflow rate at inlet decreased with the increasing of cavity depth. It indicates that the greater aspect ratio of chimney cavity width to depth (AR) is, the larger the ventilation rate at the inlet. With the increasing of AR, the average ventilation rate under different solar intensity can improve 26.7 % (AR from 1.5 to 6), 36.9 % (AR from 3/4 to 12), 23.9 % (AR from 2 to 8) for solar chimney group with one cavity, two cavities, three cavities, respectively. Thus, the natural ventilation performance for solar chimney with a small cavity depth by large width is better than that through a solar chimney with large cavity depth by small width.

As for "C" arrangements, the average maximum ventilation rate difference through solar chimney groups can achieve 43 % between C1-4 and C2-1. For the same cavity depth, the total volumetric flow rate gradually decreased with more channels in group because of less cavity width [23], such as depth 2 m in Fig. 9 (a). The main reason may be that more amount channels in group resulting in more convection heat loss due to larger side wall surface of solar chimney cavity. However, the volumetric flow rate is higher for the same cavity width by more channels. The consistent results are also found by He and Lv [36] split solar chimney into multi-channels. From Fig. 9 (b), the airflow rate across designative channel decreased with the larger channel amount in group and higher cavity depth. The difference of ventilation rate across each channel in group is small enough to neglected.

4.1.2. Model validation

Fig. 10 shows a comparison of volume flow rate predicted by Eq.(21) and numerical data as well as previous experimental data [1,5]. Before the comparison, the experimental data conducted in a 1:3 reduced scale bench by Cheng *et al.* [1] were converted to full-scale value. The average error between the present model and previous experimental data is less than 21.6 %. That probably due to the fact that the experiment used artificial light simulating the solar radiation. In fact, the energy absorbed by absorption wall is less than emission source radiation. The average error of present predictions for real building [6] is 10.9 % mainly as the up inclined ceiling of real building. The average error between the prediction and numerical modelling in a tunnel conducted by Cheng *et al.* [24] is about 16.7 %. The average error of predicted airflow rate for designative channel is 2.9 % by considering the cavity amount in the solar chimney group. The average error for total airflow rate is less 3.2 %. Totally, the predictions by the developed model Eq. (21) shows well agreement.

4.1.3. Influence of solar radiation

The influence of incident solar radiation (from 200 W/m^2 to 1400 W/m^2) on the natural ventilation through each channel is presented in

Fig. 11. The data are calculated using Eq.(21) and numerical code, that the numerical results converge well with predictions. The volumetric flow rate at inlet is improvement under more intensive solar radiation. This solar energy increases the absorber temperature that accelerates the airflow velocity through chimney cavity. The airflow rate through each channel is linear to $E^{1/3}$, this is pretty close to experimental result of $E^{0.34}$ [24] and $E^{0.33}$ [37]. The airflow rate through each channel decreases with the increasing of cavity amounts and cavity gap, and this difference value increase with greater solar energy.

4.1.4. Influence of chimney channel area

The variation of chimney cavity area influences the heat losses and airflow cross section. Fig. 12 shows the natural ventilation rate through each channel with different total chimney channel area (A_{total}) in group. The airflow rate through each channel significantly increases with larger area of chimney channel in group. The airflow rate through each channel in group shows a linear relationship with $A_{total}^{0.59}$. Consequently, the performance of natural ventilation is more sensitive to the total chimney channel area than solar intensity.

4.2. Smoke exhaustion

4.2.1. Numerical results

Fig. 13 shows the smoke exhaustion rates through each cavity in solar chimney group C1-2 and C2-2, as well corresponding natural shaft without solar energy (NC). The smoke exhaustion rate through solar chimney is slightly higher than that without solar energy but less than 6 %. That indicates the solar energy has limited effect on smoke exhaustion rate.

It is important to ascertain the variable value of the volumetric flow rate for estimating a preliminary design performance of the solar chimney group for smoke exhaustion under fire condition. Fig. 14 shows the smoke exhaustion rate under different channel aspect ratios for "C" arrangement. The volumetric flow rate is larger with stronger heat release rate. The smoke flow rate increased slightly during AR less than 3, and then decreased with the increasing of AR. The maximum smoke flow rate at inlet occurred with AR 8/3 (C3-1) under heat release rate of 3 MW and 10 MW. Moreover, for 20 MW heat release rate, the maximum smoke flow rate at the inlet occurred with AR 3 (C2-2). The plug-holing has occurred in arrangement C2-2, which means some fresh air has been entrained into the chimney that is negative for smoke exhaustion [38,39]. Therefore, the smoke exhaustion performance should be evaluated not only by volumetric flow rate but also considering the plug-holing.

The phenomenon of the plug-holing can be well indicated using temperature distribution, as shown in Fig. 15. The temperature distribution inside solar chimney centerline is plotted with 2 m cavity depth. For a given channel amounts in group, the plug-holing was more obvious with increasing of cavity depth (smaller AR). Therefore, divided channel into several small ones can improve the smoke exhaustion efficiency, this phenomenon keeps consistent with result of shaft smoke exhaust [34,35]. From temperature profile, the plug-holing has not occurred with arrangement C3-1 under fire size 3 MW, 10 MW and 20 MW. Comprehensively, combined the construction cost and structural safety, the solar chimney group C3-1 is more appropriate. Therefore, the large AR of each chimney cavities should be considered when designing the solar chimney for tunnel smoke exhaustion [40].

4.2.2. Comparison between numerical and analytical model

Fig. 16 shows a comparison of the smoke exhaustion rates through each cavity in solar chimney group between predictions and numerical results. The predictions are also compared with previous study [24]. There is some difference between the smoke exhaustion rates predicted by the analytical model and numerical results, especially for condition C2-1–2. Under the condition of C2-1–2, the predictions are larger than the numerical data for heat release rate of 3 MW and 10 MW that mainly because of overestimate the ratio of heat release rate to buoyancy flow. The total smoke exhaustion rates are fitting well with numerical result. Totally, the predicted smoke exhaustion rates by the analytical model agree reasonably well with numerical results and previous study, even though the difference still exists for small fire 3 MW. Considering the whole performance and high turbulent smoke movement, the related difference can be acceptable.

4.2.3. Influence of chimney channel area

The influence of total chimney channel area on total smoke exhaustion rate through solar chimney group and smoke exhaustion rate through each channel is shown in Fig. 17. The smoke exhaustion rate through solar chimney with one channel in group increases most significantly, the growth rate under solar chimney with two channels and three channels is gradually slow down. The total smoke exhaustion rate through solar chimney with one channel, two channels, three channels in group increases linearly with $A_{total}^{0.92}$, $A_{total}^{0.77}$, $A_{total}^{0.70}$, respectively. Fig. 17 shows the smoke exhaustion rate through first cavity linear increases with $A_{total}^{0.92}$. The smoke exhaustion rate through second channel and third channel in group shows linear relationship with $A_{total}^{0.6}$. Totally, increased the total chimney cavity area can obtain better smoke exhaustion efficiency.

5. Conclusions

In the present study, the performance of solar chimney group arrangement in tunnel is studied for natural ventilation and smoke exhaustion. The effect of solar chimney cavity amount, aspect rate of cavity, installed position, solar radiation and total chimney area on performance of solar chimney group was investigated. The theoretical model for volumetric flow rate under natural ventilation and smoke exhaustion were developed. Major conclusions can be drawn as follows:

- Divided solar chimney into multi-channels with large AR can improve the ventilation rate up to 43 %. That the most effective way to promote the ventilation rate is designing channel with wider width and narrower depth under a given chimney channel area. The natural ventilation rate increases linearly with $E^{1/3}$ and $A^{0.59}$.
- The solar radiation only enhances the smoke exhaustion rate less than 6 % that indicates the smoke exhaustion can be implemented 24 h a day using solar chimney. The smoke exhaustion rate can significantly improve by increasing the total chimney channel area. Divided the certain chimney cavity area into several channels with less cavity depth can prevent plug-holing and raise the smoke exhaustion performance.
- A theoretical model to predict the flow rate through each channel in solar chimney groups was developed under natural ventilation and smoke exhaustion, considering the horizontally semi-parabolic temperature distribution. The predictions are fitting reasonably well with numerical modelling and previous studies under varied cavity configuration, fire size, solar radiation and solar chimney group arrangement.

To conclude, the solar chimney group with several channels design is an effective enhancement technique which contributes to the application potential of solar chimney in short urban tunnel ventilation and smoke exhaustion.

CRediT authorship contribution statement

Youbo Huang: Methodology, Formal analysis, Project administration, Supervision, Writing – original draft. **Bin Wang:** Writing – review & editing, Methodology, Data curation. **Long Shi:** Conceptualization, Writing – review & editing, Methodology, Supervision, Resources. **Hua Zhong:** Methodology, Writing – review & editing. **Bingyan Dong:** Data curation, Software, Writing – review & editing.

Declaration of Competing Interest

The authors declare that they have no known competing financial interests or personal relationships that could have appeared to influence the work reported in this paper.

Data availability

The data that has been used is confidential.

Acknowledgments

The authors acknowledge support from the National Natural Science Foundation of China (NSFC) [Grant No. 52104185, 52274235], the Research Foundation of Chongqing for graduated doctor [Grant No. CSTB2022BSXM-JCX0151], the Natural Science Foundation of Chongqing, China [Grant No. cstc2021jcyj-msxmX0919], the Science and Technology Research Program of Chongqing Municipal Education Commission [Grant No. KJQN202101527], Opening Fund of State Key Laboratory of Fire Science (HZ2023-KF07), Research Foundation of Chongqing University of Science and Technology, [Grant No. ckrc2021011, ckrc2021012], Natural Science Foundation of Sichuan Province [Grant No. 2022NSFSC0278].

Appendix A. Numerical data

Under natural ventilation, the volumetric flow rate through each chimney cavity is listed in Table A1 to Table A3.

Under fire condition, the volumetric flow rate through each cavity channel is listed in Table A4 to Table A6.

References

[1] X. Cheng, L. Shi, P. Dai, G. Zhang, H. Yang, J. Li, Study on optimizing design of solar chimney for natural ventilation and smoke exhaustion, Energy Build. 170 (2018) 145–156.
[2] Y. Yang, Z. Long, H. Cheng, J. Chen, C. Liu, M. Zhong, Experimental and numerical study of smoke temperature distribution characteristics in a sloped tunnel, Sustain. Cities Soc. 73 (2021), 103091.
[3] Y. Alarie, Toxicity of fire smoke, Crit. Rev. Toxicol. 32 (2002) 259–289.
[4] B. Xie, Y.X. Han, H. Huang, L.N. Chen, Y. Zhou, C.G. Fan, X.P. Liu, Numerical study of natural ventilation in urban shallow tunnels: Impact of shaft cross section, Sustain. Cities Soc. 42 (2018) 521–537.
[5] W.Y. Liu, M.Z. Liu, R. Chang, B. Yang, H. Cui, C.Y. Li, H. Zhang, Study on moving fire smoke characteristics and mechanical ventilation system of tunnel, Fire Saf. J. 141 (2023), 103932.
[6] L. Shi, A. Ziem, G. Zhang, J. Li, S. Setunge, Solar chimney for a real building considering both energy-saving and fire safety – a case study, Energy Build. 221 (2020), 110016.
[7] Y. Huang, X. Liu, L. Shi, B. Dong, H. Zhong, Enhancing solar chimney performance in urban tunnels: Investigating the impact factors through experimental and theoretical model analysis, Energy 282 (2023) (2023), 128329.
[8] W. Ding, Y. Minegishi, Y. Hasemi, T. Yamada, Smoke control based on a solar-assisted natural ventilation system, Build. Environ. 39 (2004) 775–782.
[9] F.F. Daghistani, Solar chimney street-lighting pole for ventilating polluted urban areas, Sustain. Cities Soc. 72 (2021), 103057.
[10] A. Vazquez-Ruiz, J.M.A. Navarro, J.F. Hinojosa, J.P. Xamán, Effect of the solar roof chimney position on heat transfer in a room, Int. J. Mech. Sci. 209 (2021), 106700.
[11] F. Nasri, F. Alqurashi, R. Nciri, C. Ali, Design and simulation of a novel solar air-conditioning system coupled with solar chimney, Sustain. Cities Soc. 40 (2018) 667–676.
[12] A.A.M. Omara, H.A. Mohammed, I.J. Al Rikabi, M.A. Abuelnour, A.A. A. Abuelnuor, Performance improvement of solar chimneys using phase change materials: A review, Sol. Energy 228 (2021) 68–88.
[13] W.Y. Li, Z.D. Li, L. Xie, Y.C. Li, T.H. Long, S. Huang, J. Lu, Z.H. Wang, Evaluation of the thermal performance of an inclined solar chimney integrated with a phase change material, Energy Build. 270 (2022), 112288.
[14] T. Miyazaki, A. Akisawa, T. Kashiwagi, The effects of solar chimneys on thermal load mitigation of office buildings under the Japanese climate, Renew. Energy 31 (2006) 987–1010.
[15] S. Jaber, S. Ajib, Optimum design of Trombe wall system in mediterranean region, Sol. Energy 85 (2011) 1891–1898.
[16] H.M. Maghrabie, et al., A review of solar chimney for natural ventilation of residential and non-residential buildings, Sustain. Energy Technol. Assessments 52 (2022), 102082.
[17] T.H. Long, N.J. Zhao, W.Y. Li, S. Wei, Y.C. Li, J. Lu, S. Huang, Z.Y. Qiao, Natural ventilation performance of solar chimney with and without earth-air heat exchanger during transition seasons, Energy 250 (2022), 123818.
[18] Y. Hou, H. Li, A. Li, Experimental and theoretical study of solar chimneys in buildings with uniform wall heat flux, Sol. Energy 193 (2019) 244–252.
[19] H. Zhang, Y. Tao, G. Zhang, J. Li, S. Setunge, L. Shi, Impacts of storey number of buildings on solar chimney performance: A theoretical and numerical approach, Energy 261 (2022), 125200.
[20] P. J. Martínez, P. Martínez, J. A. Tudela, Simulation and experimental study of residential building with north side wind tower assisted by solar chimneys, 43 (2021) 102562.
[21] G. He, D. Lv, Distributed heat absorption in a solar chimney to enhance ventilation, Sol. Energy 238 (2022) 315–326.
[22] J. Gong, K. Xian, H. Liu, L. Wai, P. Seng, A novel staggered split absorber design for enhanced solar chimney performance, Build. Environ. 224 (2022), 109569.
[23] M.A. Hosien, S.M. Selim, Effects of the geometrical and operational parameters and alternative outer cover materials on the performance of solar chimney used for natural ventilation, Energy Build. 138 (2017) 355–367.
[24] X. Cheng, Z.C. Shi, K. Nguyen, L.H. Zhang, Y. Zhou, G.M. Zhang, J.H. Wang, L. Shi, Solar chimney in tunnel considering energy-saving and fire safety, Energy 210 (2020), 118601.
[25] X. Jiang, Y. Xiang, Z. Wang, Y. Mao, H. Park, A numerical study on the effect of the shaft group arrangement on the natural ventilation performance in tunnel fires, Tunn. Undergr. Sp. Technol. 103 (2020), 103464.
[26] H. Wan, Z. Gao, J. Han, J. Ji, M. Ye, Y. Zhang, A numerical study on smoke back-layering length and inlet air velocity of fires in an inclined tunnel under natural ventilation with a vertical shaft, Int. J. Therm. Sci. 138 (2019) 293–303.
[27] Q. Guo, Y. Zhen, H. Ingason, Z. Yan, H. Zhu, Theoretical and numerical study on mass flow rates of smoke exhausted from short vertical shafts in naturally ventilated urban road tunnel fires, Tunn. Undergr. Sp. Technol. 111 (2021), 103782.
[28] L. Shi, Theoretical models for wall solar chimney under cooling and heating modes considering room configuration, Energy 165 (2018) 925–938.
[29] A. Sengupta, D.P. Mishra, S.K. Sarangi, Computational performance analysis of a solar chimney using surface modifications of the absorber plate, Renew. Energy 185 (2022) 1095–1109.
[30] H.Y. Wang, C.W. Lei, A numerical investigation of combined solar chimney and water wall for building ventilation and thermal comfort, Build. Environ. 171 (2020), 106616.
[31] S. Suhendri, M. Hu, Y. Su, J. Darkwa, S. Riffat, Parametric study of a novel combination of solar chimney and radiative cooling cavity for natural ventilation enhancement in residential buildings, Build. Environ. 225 (2022), 109648.
[32] Y. Zhen, B. Lei, H. Ingason, The maximum temperature of buoyancy-driven smoke flow beneath the ceiling in tunnel fires, Fire Saf. J. 46 (2011) 204–210.
[33] J. P. Kunsch, Simple model for control of fire gases in a ventilated tunnel, 37 (2002) 67–81.
[34] Y. Oka, H. Oka, Velocity and temperature attenuation of a ceiling-jet along a horizontal tunnel with a flat ceiling and natural ventilation, Tunn. Undergr. Sp. Technol. 56 (2016) 79–89.
[35] O.F. Zhao, W. Zhang, L.Z. Xie, W. Wang, M. Chen, Z.H. Li, J.H. Li, X. Wu, X. D. Zeng, S.M. Du, Investigation of indoor environment and thermal comfort of building installed with bifacial PV modules, Sustain. Cities Soc. 76 (2022), 103463.
[36] G. He, Q. Wu, Z. Li, W. Ge, D. Lv, L. Cong, Ventilation performance of solar chimney in a test house: Field measurement and validation of plume model, Build. Environ. 193 (2021), 107648.
[37] Y. Tao, X. Fang, M.Y.L. Chew, L. Zhang, J. Tu, L. Shi, Predicting airflow in naturally ventilated double-skin facades: theoretical analysis and modelling, Renew. Energy 179 (2021) 1940–1954.
[38] J. Ji, J. Y. Han, C. G. Fan, Z. H. Gao, J. H. Sun, Influence of cross-sectional area and aspect ratio of shaft on natural ventilation in urban road tunnel, 67 (2013) 420–431.
[39] C. G. Fan, J. Ji, W. Wang, J. H. Sun, Effects of vertical shaft arrangement on natural ventilation performance during tunnel fires, 73 (2014) 158–169.
[40] Q. Guo, H. Zhu, Z. Yan, Y. Zhang, Y. Zhang, T. Huang, Experimental studies on the gas temperature and smoke back-layering length of fires in a shallow urban road tunnel with large cross-sectional vertical shafts, Tunn. Undergr. Sp. Technol. 83 (2018) 565–576.